



DEPARTMENT OF  
ENERGY, MINES AND RESOURCES  
MINES BRANCH  
OTTAWA

*HYDROGEN-ATMOSPHERE GALVANIZING  
OF IRON-BASE ALLOYS*

J. J. SEBISTY AND G. E. RUDDLE

PHYSICAL METALLURGY DIVISION

DECEMBER 1972



© Crown Copyrights reserved

Available by mail from Information Canada, Ottawa,  
and at the following Information Canada bookshops:

HALIFAX  
1687 Barrington Street

MONTREAL  
640 St. Catherine Street West

OTTAWA  
171 Slater Street

TORONTO  
221 Yonge Street

WINNIPEG  
393 Portage Avenue

VANCOUVER  
800 Granville Street

or through your bookseller

Price 75 cents      Catalogue No. M38-1/255

Price subject to change without notice

Information Canada  
Ottawa, 1973

Mines Branch Research Report R255

HYDROGEN-ATMOSPHERE GALVANIZING OF IRON-BASE ALLOYS

by

J. J. Sebisty\* and G. E. Ruddle\*

- - - - -

ABSTRACT

Series of iron-base alloys containing manganese, phosphorus and silicon were galvanized in a hydrogen-atmosphere apparatus over a range of time and temperature conditions.

Manganese in amounts of 0.17, 0.50 and 1.17% failed to exert any prominent effect on coating formation.

Phosphorus-containing alloys (0.01, 0.042, 0.069, and 1.1% P), exhibited relatively high galvanizing reactivity which was characterized by increasing unevenness in iron-zinc alloy growth with increasing phosphorus content and immersion time.

The reactivity of the silicon-containing alloys (0.03, 0.08, 0.21, 0.91 and 3.4% Si) generally followed established behaviour but with some significant anomalies. Most notable was a reaction rate inversion in going from the normal galvanizing temperature of 450°C (840°F) to 470°C (880°F). At this higher temperature, the coating microstructures were significantly altered towards thinner, more compact, iron-zinc alloy layers.

---

\* Research Scientist, Non-Ferrous Metals Section, Physical Metallurgy Division, Mines Branch, Department of Energy, Mines and Resources, Ottawa, Canada.

Direction des mines  
Rapport de recherches R255

LA GALVANISATION DES ALLIAGES À BASE  
DE FER DANS UN APPAREIL AVEC UNE ATMOSPHERE D'HYDROGÈNE

par

J.J. Sebisty\* et G.E. Ruddle\*

RÉSUMÉ

Les auteurs ont galvanisé des alliages à base de fer, contenant du manganèse, du phosphore et du silicium dans un appareil avec une atmosphère d'hydrogène, sous différentes conditions de temps et de température.

Des montants de manganèse de 0.17, 0.50, et 1.17% n'ont pas exercé d'effets importants sur la formation du revêtement.

Les alliages contenant du phosphore (0.01, 0.042, 0.069 et 1.1%P) ont montré une réactivité relativement élevée de galvanisation qui était caractérisée par une inégalité croissante dans le développement de l'alliage fer-zinc avec une teneur en phosphore et une période d'immersion grandissantes

La réactivité des alliages contenant du silicium (0.03, 0.08, 0.21, 0.91 et 3.4%S) a généralement suivi le procédé établi mais avec quelques anomalies significatives. L'anomalie la plus remarquable a été l'inversion de la vitesse de réaction en allant de 450°C (la température normale de galvanisation) à 470°C. A 470°C les microstructures du revêtement ont été changées significativement pour donner des couches d'alliage fer-zinc plus minces et plus compactes.

---

\*Chercheurs scientifiques, Section des métaux non ferreux, Division de la métallurgie physique, Direction des mines, ministère de l'Énergie, des Mines et des Ressources, Ottawa, Canada.

CONTENTS

	<u>Page</u>
Abstract . . . . .	i
Résumé . . . . .	ii
Introduction . . . . .	1
Materials . . . . .	1
Sample Preparation . . . . .	2
Galvanizing Experiments . . . . .	2
Results and Discussion . . . . .	3
Manganese-Containing Alloys and Electrolytic Iron . . . . .	4
Phosphorus-Containing Alloys . . . . .	4
Silicon-Containing Alloys . . . . .	5
Summary and Conclusions . . . . .	7
References . . . . .	9
Tables 1-2 . . . . .	10, 11
Figures 1-13 . . . . .	12- 21

TABLES

<u>No.</u>		<u>Page</u>
1.	Chemical Composition of Iron-Base Alloys (%) . . . . .	10
2.	Galvanizing Experiments . . . . .	11

FIGURES

1.	Microstructures of electrolytic iron and iron-base alloys containing manganese and phosphorus . . . . .	12
2.	Microstructures of iron-base alloys containing silicon . . . . .	13
3.	Iron weight loss versus immersion time for electrolytic iron at temperatures indicated. . . . .	14
4.	Iron weight loss versus immersion time at 450°C(840°F) for iron-base alloys containing manganese and phosphorus . . . . .	14
5.	Iron weight loss versus immersion time for iron-base alloys containing silicon at temperatures indicated . . . . .	15
6.	Iron weight loss versus silicon content at 450°C(840°F) for immersion times indicated. . . . .	16
7.	Microstructures of coatings on electrolytic iron at different temperatures. . . . .	17
8.	Microstructures of coatings on manganese-containing alloys at 450°C (840°F) . . . . .	17
9.	Microstructures of coatings on phosphorus-containing alloys at 450°C (840°F). . . . .	18
10.	Microstructures of coatings on silicon-containing alloys at 450°C (840°F) . . . . .	19
11.	Microstructures of coatings on 0.08% Si alloy at different temperatures . . . . .	20
12.	Microstructures of coatings on 0.21% Si alloy at different temperatures . . . . .	21
13.	Microstructures of coatings on 3.4% Si alloy at different temperatures. . . . .	21

## INTRODUCTION

Study of the kinetics of the galvanizing process represents one in the continuing series of projects done at the Mines Branch in co-operation with the Canadian Galvanizing Research Association (formerly, Galvanizing Subcommittee, Canadian Zinc and Lead Research Committee) and the International Lead Zinc Research Organization, Inc. (ILZRO). The principal aim has been to investigate parameters which influence and control the reactivity of ferrous metal surfaces in molten zinc.

Initial work on the project was concerned with the design, construction, and commissioning of an apparatus for galvanizing in a filtered zinc bath maintained in a hydrogen atmosphere (1) (2). Elimination of conventional pickling and fluxing pretreatments and sample immersion through a clean oxide-free surface are principal features of the method. The apparatus and its operation are described in a separate report (3).

The primary experimental effort utilizing the hydrogen apparatus dealt with galvanizing tests on three groups of iron-base alloys containing additions of silicon, manganese, and phosphorus. This was to serve as a preliminary study preceding a more comprehensive program on a range of experimental steels to be prepared from the basic alloys. This intention had to be abandoned when ILZRO support for the project was discontinued in 1971. Nevertheless, the work done on the three groups of alloys is considered to be of some value and interest, and, therefore, the experiments made are described in this report.

## EXPERIMENTAL PROCEDURE

### Materials

The iron-base materials purchased from the British Iron and Steel Research Association comprised five silicon-containing alloys (0.03 to 3.4% Si), three manganese-containing alloys (0.17 to 1.17% Mn), four phosphorus-containing alloys (0.01 to 1.1% P), and a grade of electrolytic iron. The chemical compositions are given in Table 1. The alloys had been prepared by vacuum melting using electrolytic iron as a base and by hot finishing to 1-in. -diameter rods except for the phosphorus-containing group. The latter cracked on rolling because of hot shortness and were supplied as 3-in. cubes in the as-cast condition. Microstructures of the various materials are illustrated in Figures 1 and 2.



### Sample Preparation

The alloys were machined to discs 0.75 in. in diameter and surface ground to a thickness of 0.040 in. with a 60-grit aluminum oxide wheel of medium hardness (Norton 38A 60-K8VBE). Edge burrs from grinding and from drilling of suspension holes were removed by vibratory polishing for 2 hr on 600-grit silicon carbide paper lubricated with kerosene. After vapor degreasing, the discs were vacuum annealed for 0.5 hr at 940°C (1725°F) and furnace cooled. To further ensure a uniform surface condition before galvanizing, the discs were air-oxidized at 200°C (390°F) to a light straw-temper colour. The times were between 1 and 12 hr depending on the alloy composition. In blank tests made, the weight gain due to oxidation was found to be negligible.

The final pretreatment step was an integral part of the galvanizing operation and entailed reduction of the oxidized sample surface in purified hydrogen. This was done in two stages for times of 0.75 and 1 hr at a sample temperature of 450°C (840°F). It is of interest to note that the high silicon (3.4%) alloy presented no difficulties in galvanizing. In other work (4), conventional galvanizing of similar high-silicon materials required special pretreatment by electropolishing with perchloric acid solution or by hydrofluoric acid pickling to produce satisfactory coatings.

### Galvanizing Experiments

Details of the galvanizing operation in the hydrogen-atmosphere apparatus are given elsewhere (3). For loading in the chamber, the sample discs were wired together in pairs, one above the other. The lower pre-weighed disc of each pair provided a sample for measurement of the iron weight loss to determine the amount of iron reacting with zinc in the galvanizing reaction. The twenty galvanizing runs made are listed in Table 2. Samples of each of the thirteen materials were immersed for 1, 2½, 5, and 10 min in special high-grade (99.99%) zinc at a nominal bath temperature of 450°C (840°F). Additional runs made at 430°C (805°F) and 470°C (880°F) were intended to obtain further information on the behaviour of some of the silicon-containing alloys (0.08, 0.21 and 3.4% Si) and of the electrolytic iron.

As previously described (1), the initial runs (No. 45, 46, 49, 50 and 51) were made using a simultaneous filtering-dipping technique. The sample discs were positioned so as to be covered by the rising bath of filtered zinc as the filtering process proceeded. This immersion technique was subsequently discontinued because the initial chilling effect of the filtering crucible presented difficulties in achieving the specific bath temperature desired. In all subsequent runs, the samples were manually lowered, one pair at a time, several minutes after filtering was completed and the bath temperature had stabilized. Sample contamination from pick-up of oxides which gradually



formed on the filtered bath was avoided by immersion before significant oxidation had taken place. With both techniques, therefore, the objective of immersing the samples through a clean bath surface was essentially achieved.

The samples were manually withdrawn, rotated rapidly to remove excess zinc, and raised to the coolest zone in the apparatus chamber where the temperature was of the order of 175°C (345°F). After melt furnace shut-down, the temperature in this zone drops to 145°C (295°F) within 5 min and at a slower rate thereafter of about 3°C (6°F) or less per min. These measurements were made without hydrogen circulation. More rapid cooling was probably achieved in the actual galvanizing runs during which hydrogen flow was maintained; continued iron-zinc reaction during the cooling period was therefore presumed to be negligible.

Evaluation of the galvanizing behaviour was made by metallographic examination on one of each pair of samples and by measurement of the iron weight loss on the other. Metallographic polishing and etching followed established procedures. Stripping of the coatings for the weight loss tests presented difficulties because of the different chemical reactivity of the substrate materials and because of the large blob of excess zinc remaining around the bottom edge of the samples. The principal problem was to minimize experimental error as a result of earlier exposure and attack of the substrate at more thinly-coated areas. Experiments were made with a reagent (5) which was claimed to selectively remove the outer zinc layer without attacking the underlying iron-zinc alloy layers. The procedure was found to be very slow and also required frequent reactivation of the reagent mixture. The alternative approach was adopted of using stripping solutions of different strength as follows: standard HCl-SbCl<sub>3</sub> solution for the electrolytic iron and iron-manganese samples; a solution of 1 HCl to 5 H<sub>2</sub>O, by volume, for the iron-phosphorus samples; a solution of 1 HCl to 9 H<sub>2</sub>O, by volume, for the iron-silicon samples. Blank tests confirmed that, under the above conditions, there was no significant attack of the bare substrate materials.

## RESULTS AND DISCUSSION

The results of the iron weight loss tests are graphically presented in Figures 3 to 6 and typical microstructures for all the coatings produced are illustrated in Figures 7 to 13. Because of experimental error, weight loss results for the 0.01% P series of tests are not available. Also, suspension failure prevented retrieval, from the bath, of the 0.08% Si samples to be dipped for 10 min.

### Manganese-Containing Alloys and Electrolytic Iron

No significant coating effects were found with the manganese-containing alloys galvanized at 450°C (840°F) as indicated by Figures 4 and 8. The weight loss values and coating microstructures were practically identical at the different manganese levels. They were also more or less indistinguishable from the results for the electrolytic iron at the same temperature (Figures 3 and 7).

A minor change of interest was the apparent tendency to more even growth of the  $\zeta$  and  $\delta_1$  layers, notably at the 0.17% and 0.50% Mn levels. Local irregularities in growth as commonly found with plain-carbon mild steels were more prominent with the electrolytic iron, especially at 450°C (840°F), as shown in Figure 7. Better uniformity was indicated at both the lower and higher temperatures of 430°C (805°F) and 470°C (880°F). Figure 7 also illustrates the changing growth characteristics of the  $\zeta$  and  $\delta_1$  layers on the electrolytic iron with increasing time and temperature, reaching the stage where the  $\delta_1$  was the predominant constituent and formed about 50% of the total coating thickness.

### Phosphorus-Containing Alloys

Relatively high reactivity and uneven coating growth were generally prominent features exhibited by the phosphorus-containing alloys (Figures 4 and 9). The  $\zeta$  phase was the predominant constituent under all conditions. Locally thicker patches of  $\zeta$ , which otherwise showed uniform and compact layer growth, were evident even at the shortest immersion time of 1 min. Growth of the adjoining  $\delta_1$  also varied from isolated crystallite formation to a thin continuous layer. Increasing the immersion time and, more particularly, the phosphorus content resulted in marked development of prominent, dome-shaped  $\zeta$  outbursts showing variable growth. At the maximum phosphorus level (1.1%), the entire surface was affected so that a continuous hill-and-valley contour was produced. The  $\delta_1$  phase formed a compact layer which also increased in thickness with immersion time. As is usual, its thickness was slightly reduced where  $\zeta$  growth was locally accelerated. A very thin  $\Gamma$  layer was generally present only in the structures immersed for the longest time (10 min).

The trend of the weight loss curves in Figure 4 suggests that the overall reaction rate in each case conformed to parabolic kinetics. Nevertheless, a linear reaction mode at the sites of the  $\zeta$  outbursts is well defined in the microstructures. The usual reason for such accelerated local attack, namely, direct access of zinc to the  $\delta_1$  layer, would not appear to be responsible. This follows from the fine grained and generally dense-packed  $\zeta$  outbursts except as noted below. An alternative explanation offered by Harvey (6) suggests that such outbursts are primarily related to local impurity concentrations (in this case, of phosphorus) in the substrate. Possible consequences are local

slowing down of diffusion in the substrate or build-up of the impurity in the  $\delta_1$  layer to alter its stable growth characteristics. He proposes that either or both of these effects could promote sudden transformation of "palisade"  $\delta_1$  to  $\zeta$ , which are of similar composition. Once initiated, rapid transformation of  $\delta_1$  as well as  $\Gamma$  to  $\zeta$  proceed unhindered in a linear reaction mode. This sequence of events remains to be conclusively confirmed but appears to be supported, in the present case, not only by the increasing outburst activity with increasing phosphorus content and immersion time but by the growth characteristics of the individual iron - zinc alloy layers in the microstructures. As noted later, a somewhat similar phenomenon was found with the 3.4% Si alloy.

Figure 4 also indicates that galvanizing reactivity was a maximum at 0.069% P and the further increase to 1.1% reduced the measured iron loss at all immersion times. The microstructures for the former in Figure 9 are in accord with the hypothesis (6) that compactness of the  $\zeta$  layer is eventually destroyed because of prior rapid growth. This facilitates the reaction between liquid zinc and  $\delta_1$  which, in turn, would be expected to accelerate  $\zeta$  formation and increase the total iron loss. In contrast, relatively dense packing was retained within the massive  $\zeta$  formations at 1.1% P and the better diffusion barrier provided must have restricted iron movement. Why the more advanced break-away stage was reached at 0.069% instead of 1.1% P is not known. However, an uneven distribution of phosphorus is not an exceptional occurrence and it will be recalled that this group of alloys was supplied in the as-cast condition and annealed without prior working.

The cross-over of the curves in Figure 4 for the 0.042% and 1.1% P alloys at 10 min immersion is not considered significant. Experimental error could have been involved since only single weight loss determinations were made. The consistent but unusually high reactivity of the 0.01% P alloy (Figure 9) is equally difficult to explain. It is unknown to what extent either the large grain size of this material or the hydrogen surface pretreatment were responsible.

### Silicon-Containing Alloys

Considering the lower reactivity silicon-containing materials first, Figures 5 and 10 indicate that the 0.03% Si alloy at 450°C (840°F) behaved much like electrolytic iron, although increased iron-zinc alloy growth, especially of the  $\zeta$  phase, resulted in generally higher iron losses. Otherwise, both series of coating microstructures (Figures 7 and 10) showed basically similar features with all of the iron-zinc phases being present in normal layer formation. At the opposite composition extreme of 3.4% Si, the well-known very low iron-zinc reactivity, synonymous with a high silicon content, was clearly defined at 450°C (840°F). The iron loss values (Figure 5) were well below those for the electrolytic iron and were reflected in extremely thin and uniform coatings composed of only  $\zeta$  and  $\delta_1$  as shown in Figure 10.

The reasons for this high-silicon effect have never been established. It is the more unusual because of the deterioration to non-uniform iron-zinc alloy growth at the higher temperature of 470°C (880°F). Figure 13 illustrates typical microstructures which duplicate the hill-and-valley  $\zeta$  contouring found with the phosphorus-containing alloys. Similar segregation phenomena may be applicable but in the opposite sense to that discussed in the previous section, i. e., local areas contained less than the bulk silicon content of 3.4% and were accordingly more reactive. As in the phosphorus series, it is again evident that direct reaction of liquid zinc with  $\delta_1$  was not involved in formation of the  $\zeta$  outbursts. Noteworthy as well was the re-appearance of the  $\Gamma$  phase as a thin continuous layer at all immersion times at this higher temperature.

The high iron-zinc reactivity usually associated with silicon was reflected in the behaviour of the remaining alloys (0.08, 0.21 and 0.91% Si) at 450°C (840°F). Different reaction rates, more or less conforming to linear kinetics, were apparent and were related to two distinctly different iron-zinc alloy growth modes. Unusually, the reactivity was a maximum at 0.08% Si, being significantly higher than at 0.91%, and much more so than at 0.21%. The respective weight loss changes plotted against immersion time are shown in Figure 5, and against silicon content for the 450°C (840°F) series of tests in Figure 6. The latter highlights the increasingly pronounced reactivity peak with increasing immersion time at 0.08% Si. The plots in Figure 5 also show significant temperature anomalies which are discussed later.

The thick coatings on the 0.08% Si alloy at 450°C (840°F) were made up almost entirely of very fine  $\zeta$  crystals as illustrated in Figure 10. This granular mixture was bounded by an extremely thin and continuous  $\delta_1$  layer and there was no evidence of the  $\Gamma$  phase. The corresponding coatings on the 0.21 and 0.91% Si alloys (Figure 10) were more characteristic of those commonly found in commercial galvanizing of silicon-containing steels. A principal feature was rapid  $\zeta$  growth which assumed distinct columnar growth of individual crystals even at short immersion times, and more so with increasing silicon content. The accompanying  $\delta_1$  growth was also irregular. Increasing immersion times eventually produced a loosely-packed free-floating mass of coarse  $\zeta$  crystals embedded in a zinc matrix. An idiomorphic growth habit was suggested. Irregular  $\delta_1$  growth was maintained throughout and, wherever there was direct contact with zinc, the reaction resulted in break-up of the  $\delta_1$  into masses of finely-granulated crystals. Underneath such areas, a layer of variable thickness of high-iron "coherent"  $\delta_1$  remained as a compact cover on the substrate surface. The  $\Gamma$  iron-zinc layer was again absent.

As is common with commercial coatings of this type, the thicker experimental coatings generally showed a fringe band of small  $\zeta$  crystals adjoining the outer zinc layer. The relatively smooth boundary thereby presented minimizes zinc drag-out and partly accounts for the thin outer zinc



layer which is generally found with this class of coating.

Of particular interest is the anomalous temperature effect evident in Figure 5 at the 0.08 and 0.21% Si levels. Under all known galvanizing conditions, iron-zinc reactivity increases with increasing temperature in the lower parabolic and the linear reaction regions, i. e., below 515°C (960°F). This normal response was apparent in going from 430°C (805°F) to 450°C (840°F) but the further increase to 470°C (880°F) produced a significantly lower weight loss which increased progressively with immersion time. With 0.08% Si, the weight losses dropped to intermediate levels between the two lower temperatures whereas, at 0.21%, the indicated reactivity was least at the highest temperature. In other words, maximum reactivity for both materials occurred at the so-called normal galvanizing temperature of 450°C (840°F).

Although the recorded weight loss reductions were not large, they represented relatively major coating microstructure modifications. Appreciable reductions in thickness of the iron-zinc alloy structure as a whole were well defined (Figures 11 and 12). With the 0.08% Si material, distinct coarsening of the  $\zeta$  crystals and minimal increase in  $\delta_1$  growth were also apparent at the higher temperature. At 0.21% Si, the effects were more striking, especially at the longer immersion times. As Figure 12 shows, the very uneven and open structure at 450°C (840°F) was replaced by closely packed uniform growth of columnar  $\zeta$  crystals. Local breakdown of  $\delta_1$  by direct contact with zinc was not evident and thickness uniformity of the iron-zinc alloy structure as a whole was thereby greatly improved. The reductions in coating thickness achieved in this case at 470°C (880°F) are especially noteworthy.

A brief reference to such reduced reactivity with increasing temperature was made in previous work (4) with a commercial silicon-containing steel. Its confirmation in the present limited tests suggests it is a real effect which represents a further unexplained anomaly associated with galvanizing of silicon-containing steels. Because of its potential implications in commercial galvanizing, a more intensive program of tests to investigate this phenomena has been undertaken as part of ILZRO Project ZM-178 (Galvanizing of Silicon-Containing Steels).

## SUMMARY AND CONCLUSIONS

Galvanizing in a hydrogen-atmosphere environment of iron-base materials containing manganese, phosphorus and silicon produced a variety of effects.

Manganese at levels of 0.17, 0.50, and 1.17% had no significant effect on coating formation except to the extent of promoting more even growth of

the  $\zeta$  and  $\delta_1$  iron-zinc alloy layers. Local irregularities in growth which are frequently observed with plain-carbon mild steel were thereby minimized.

Relatively high galvanizing reactivity and uneven iron-zinc alloy growth were principal characteristics of the phosphorus-containing alloys (0.01, 0.042, 0.069, 1.1%). Increase in phosphorus content as well as immersion time resulted in marked growth of prominent dome-shaped  $\zeta$  - phase outbursts which are possibly related to phosphorus segregation in the substrate or within the growing iron-zinc alloy layers during galvanizing.

Galvanizing reactivity of the silicon-containing alloys varied widely in accordance with established behaviour but significant anomalous effects, either less well known or previously unreported, were revealed.

There was a moderate increase in reactivity even at 0.03% Si but the conventional, compact, layered-structure of iron-zinc phases was retained.

At the opposite extreme of 3.4% Si, very low reactivity synonymous with a high silicon content was well defined at 450°C (840°F). The coatings were extremely thin and iron weight losses were well below those for electrolytic iron. Increasing the temperature to 470°C (880°F) produced dome-shaped  $\zeta$  outbursts not unlike those caused by phosphorus, and similar segregation phenomena, in this case involving silicon, were probably responsible.

At the normal galvanizing temperature of 450°C (840°F), the intermediate silicon levels exhibited different degrees of high reactivity. Maximum effects were recorded at 0.08% Si and were related to pronounced growth of a fine-grained  $\zeta$  structure sometimes described as "beard formation". The reactivity was significantly lower at 0.91%, still more so at 0.21%, and the respective coating microstructures were most nearly representative of commercial coatings on silicon-containing steels. At lengthy immersion times particularly, they consisted largely of small to very coarse  $\zeta$  crystals free-floating in a zinc matrix. Accompanying features were break-up of  $\delta_1$  into a fine granular mass, where it was in direct contact with zinc, and absence of  $\Gamma$  under all conditions tried.

The 0.08 and 0.21% Si alloys revealed a significant reactivity inversion between 450°C (840°F) and 470°C (880°F). The effects were not large in terms of iron weight loss but reflected major microstructural modifications towards thinner, more compact, iron-zinc alloy structures. It is premature to speculate on the practical implications of this anomalous behaviour, so a more intensive study is being attempted.

REFERENCES

1. Sebisty, J.J., Brown, W.N. and Palmer, R.H. (1970), Physical Metallurgy Division Internal Reports PM-R-70-2 and PM-R-70-11, Mines Branch, Department of Energy, Mines and Resources, Ottawa.
2. Sebisty, J.J., and Ruddle, G.E. (1971), Physical Metallurgy Division Internal Report PM-R-71-13, Mines Branch, Department of Energy, Mines and Resources, Ottawa.
3. Ruddle, G.E., and Sebisty, J.J. (1972), Mines Branch Research Report R 247, Mines Branch, Department of Energy, Mines and Resources, Ottawa.
4. Hershman, A. A., and Neemuchwala, N.D. (March 1966), BNFMRA Report No. A-1594.
5. Kokorin, G.A. (1969), Sb. Tr. Tsent. Nauch, Issled. Inst. Chern. Met. (USSR), No. 66, 87-91.
6. Harvey, G.J. (1962), J. Aust. Inst. Metals 7, 17.

- - - -

TABLE 1

Chemical Composition of Iron-Base Alloys (%)

Material	C	Si	Mn	P	S	Al	O	H	N
<u>Electrolytic Iron</u>									
AH28	.0025	.004	.004	.001	.003	.0045	.0008	<.0001	.0012
<u>Iron-Manganese Alloys</u>									
K1145	.005	<.006	.17	<.004	<.01		.02		
K1144	.008	"	.50	"	"		.02		
K1146	.004	"	1.17	"	"		.017		
<u>Iron-Phosphorus Alloys</u>									
K1224	.01	<.006	<.01	.01	<.007		.003		
K1228	.004	"	"	.042	"		.02		
K1225	.006	"	"	.069	"		.005		
K1226	.004	"	"	1.10	"		.007		
<u>Iron-Silicon Alloys</u>									
K1147	.005	.03	<.01	<.004	<.01		.01		
K1148	.006	.08	"	"	<.01		.006		
K1149	.007	.21	"	"	<.01		.004		
K1223	.02	.91	"	"	<.007		.003		
K1151	.007	3.40	"	"	<.01		.003		



TABLE 2

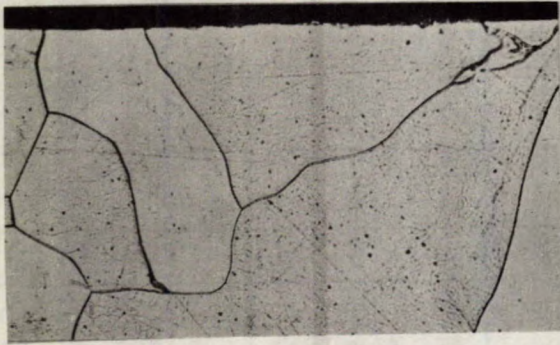
Galvanizing Experiments

Run and Sample No.	Iron-base Material*	Galvanizing **	
		Temp - °C(°F)	Time (min)
61 (1 to 8)	AH28 (electrolytic iron)	430 (805)	1, 2 $\frac{1}{2}$ , 5, 10
60 (1 to 8)	"	450 (840)	1, 2 $\frac{1}{2}$ , 5, 10
64 (1 to 8)	"	470 (880)	1, 2 $\frac{1}{2}$ , 5, 10
53 (1 to 8)	K1145 (Fe + 0.17% Mn)	455 (850)	1, 2 $\frac{1}{2}$ , 5, 10
54 (1 to 8)	K1144 (Fe + 0.50% Mn)	450 (840)	1, 2 $\frac{1}{2}$ , 5, 10
55 (1 to 8)	K1146 (Fe + 1.17% Mn)	450 (840)	1, 2 $\frac{1}{2}$ , 5, 10
56 (1 to 8)	K1224 (Fe + 0.01% P)	450 (840)	1, 2 $\frac{1}{2}$ , 5, 10
57 (1 to 8)	K1228 (Fe + 0.042% P)	452 (845)	1, 2 $\frac{1}{2}$ , 5, 10
58 (1 to 8)	K1225 (Fe + 0.069% P)	452 (845)	1, 2 $\frac{1}{2}$ , 5, 10
59 (1 to 8)	K1226 (Fe + 1.10% P)	450 (840)	1, 2 $\frac{1}{2}$ , 5, 10
45 (1 to 8)	K1147 (Fe + 0.03% Si)	452 (845)	1, 2 $\frac{1}{2}$ , 5, 10
62 (1 to 8)	K1148 (Fe + 0.08% Si)	432 (810)	1, 2 $\frac{1}{2}$ , 5, 10
46 (1 to 6)	"	451 (845)	1, 2 $\frac{1}{2}$ , 5
65 (1 to 8)	"	470 (880)	1, 2 $\frac{1}{2}$ , 5, 10
63 (1 to 8)	K1149 (Fe + 0.21% Si)	430 (805)	1, 2 $\frac{1}{2}$ , 5, 10
49 (1 to 8)	"	451 (845)	1, 2 $\frac{1}{2}$ , 5, 10
67 (1 to 8)	"	468 (875)	1, 2 $\frac{1}{2}$ , 5, 10
50 (1 to 8)	K1223 (Fe + 0.91% Si)	448 (840)	1, 2 $\frac{1}{2}$ , 5, 10
51 (1 to 8)	K1151 (Fe + 3.4% Si)	450 (840)	1, 2 $\frac{1}{2}$ , 5, 10
66 (1 to 8)	"	470 (880)	1, 2 $\frac{1}{2}$ , 5, 10

\* 0.75 x 0.40-in. machined discs (surface ground), de-burred, vacuum annealed, pre-oxidized in air for 1 to 12 hr at 200°C (390°F), and treated in purified hydrogen for 1.5 to 2.0 hr at 450°C (840°F) before dipping.

\*\* Pairs of sample discs dipped in all cases in special high-grade (99.99%) zinc.





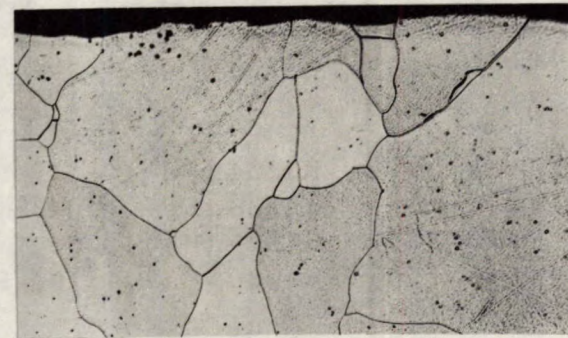
(a) Electrolytic iron



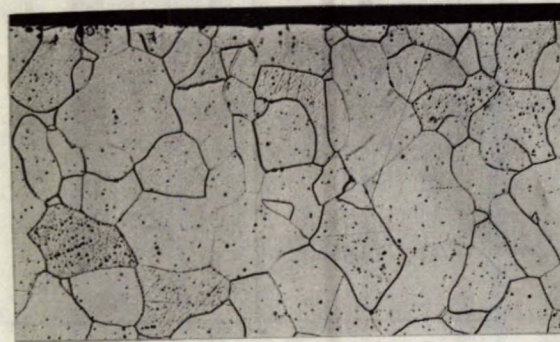
(e) 0.01% P



(b) 0.17% Mn



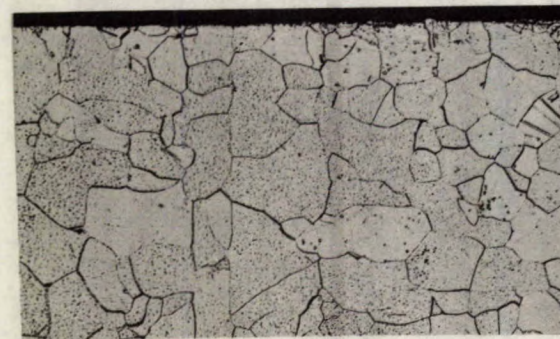
(f) 0.042% P



(c) 0.50% Mn



(g) 0.069% P



(d) 1.17% Mn



(h) 1.10% P

Figure 1. Microstructures of electrolytic iron and iron-base alloys containing manganese and phosphorus. Nital etch, X100.

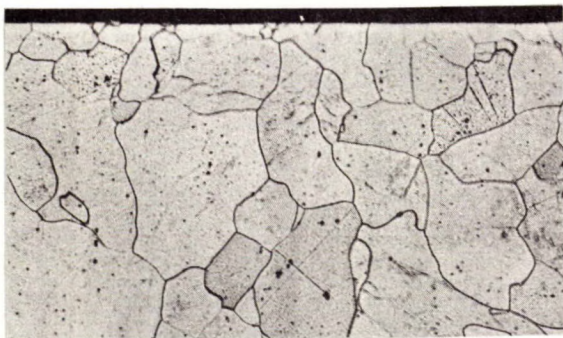




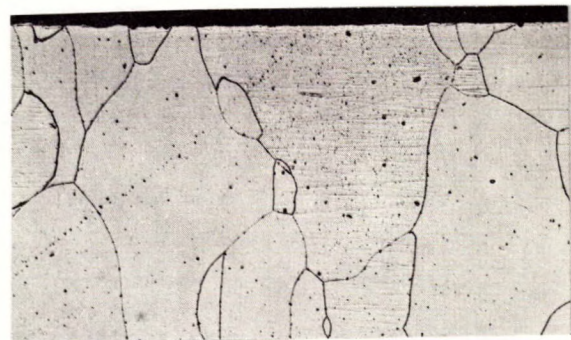
(a) 0.03% Si



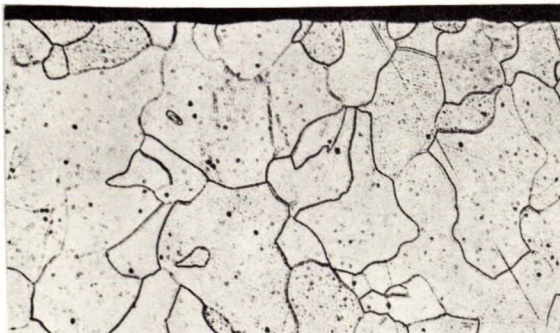
(d) 0.91% Si



(b) 0.08% Si



(e) 3.4% Si



(c) 0.21% Si

Figure 2. Microstructures of iron-base alloys containing silicon. Nital etch, X100.

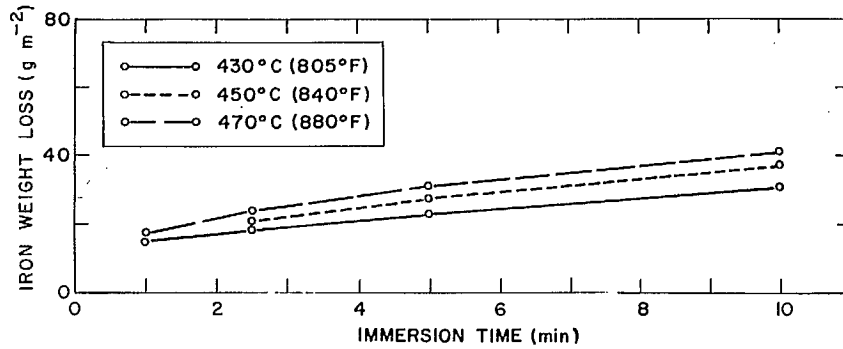


Figure 3. Iron weight loss versus immersion time for electrolytic iron at temperatures indicated.

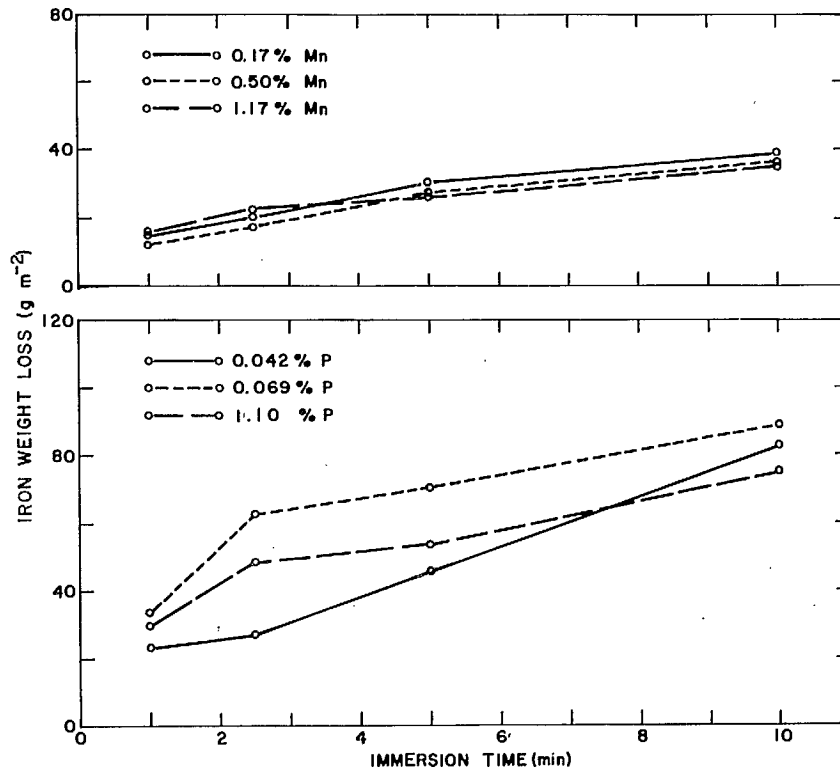


Figure 4. Iron weight loss versus immersion time at 450°C (840°F) for iron-base alloys containing manganese and phosphorus.



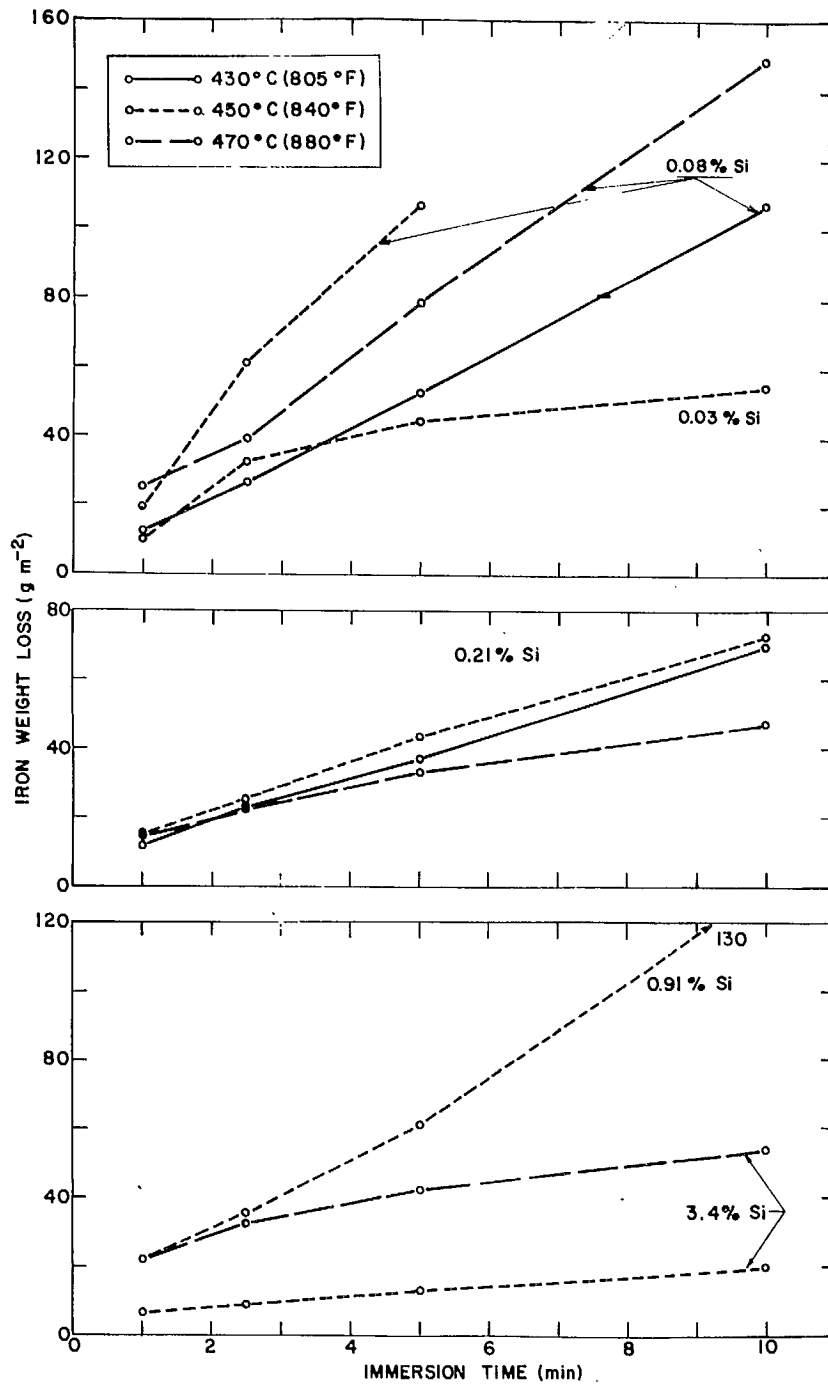


Figure 5. Iron weight loss versus immersion time for iron-base alloys containing silicon at temperatures indicated.

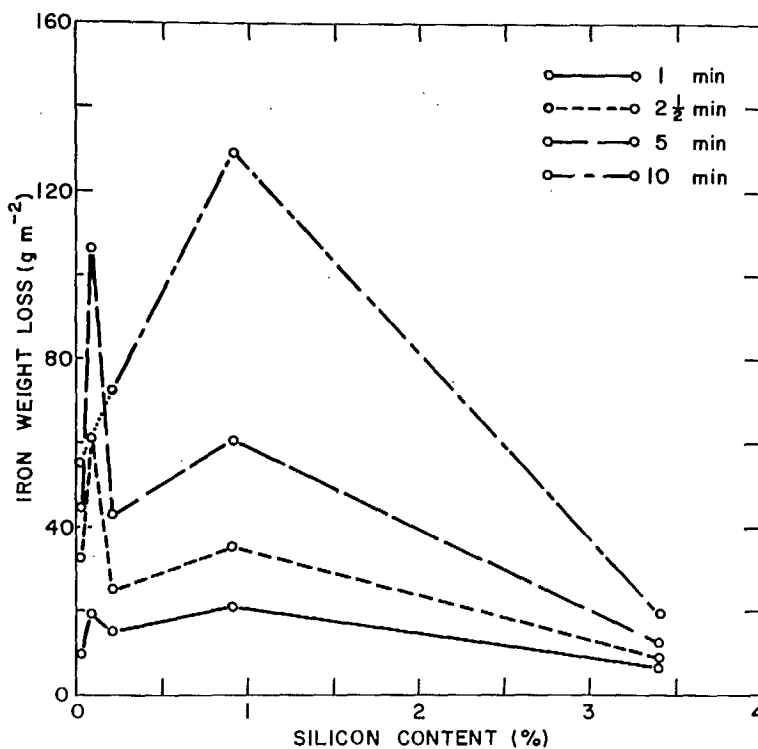


Figure 6. Iron weight loss versus silicon content at 450°C (840°F) for immersion times indicated.

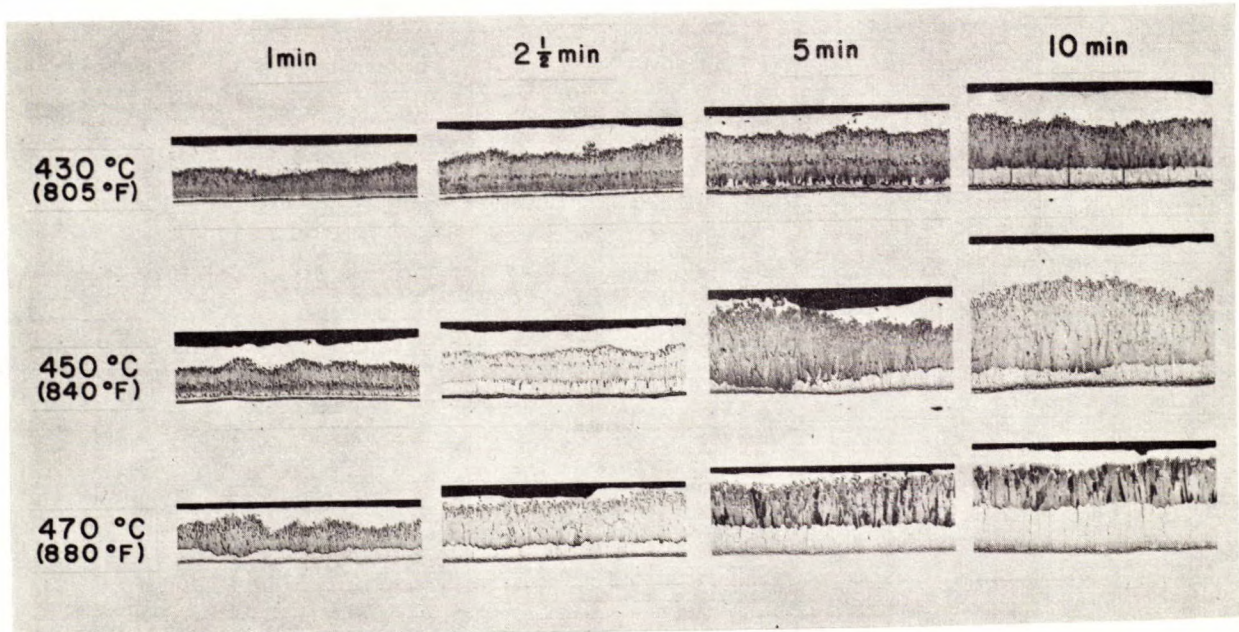


Figure 7. Microstructures of coatings on electrolytic iron at different temperatures. Magnification reduced to 190X in reproduction.

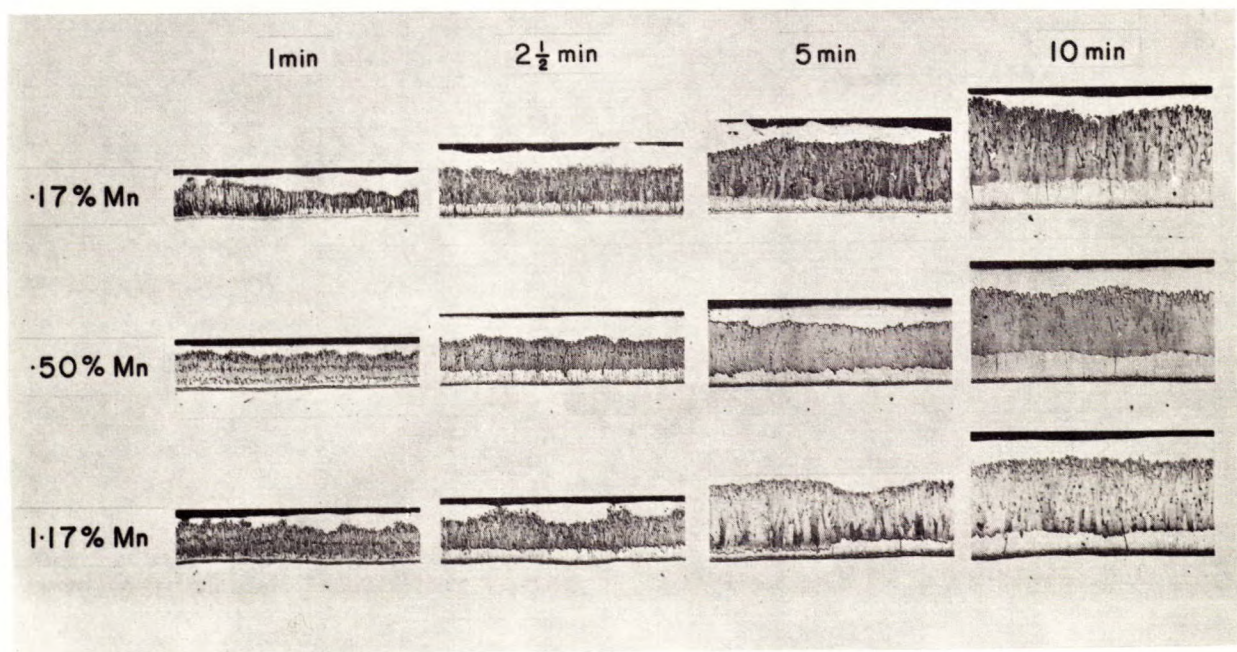


Figure 8. Microstructures of coatings on manganese-containing alloys at 450°C (840°F). Magnification reduced to 185X in reproduction.



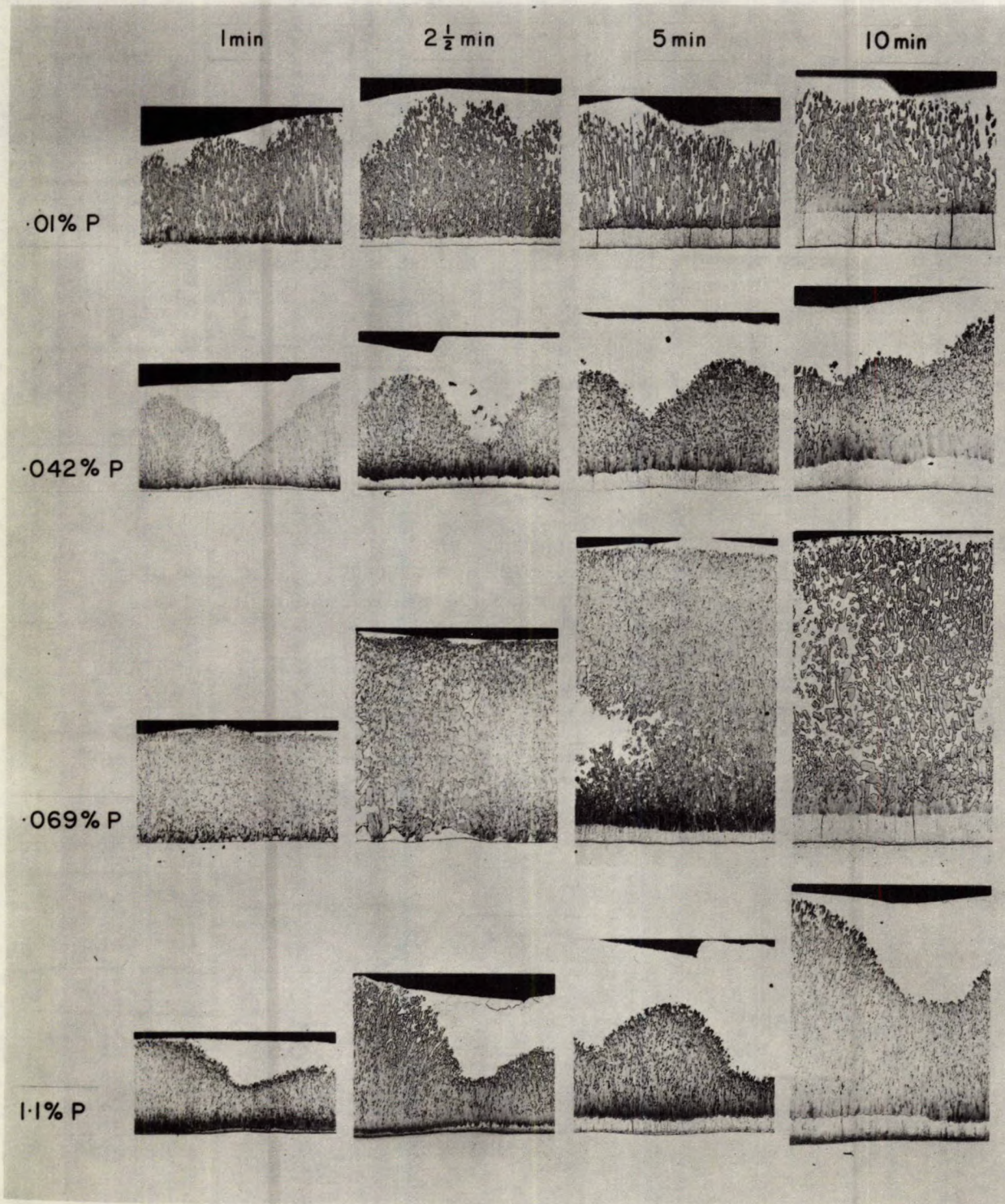
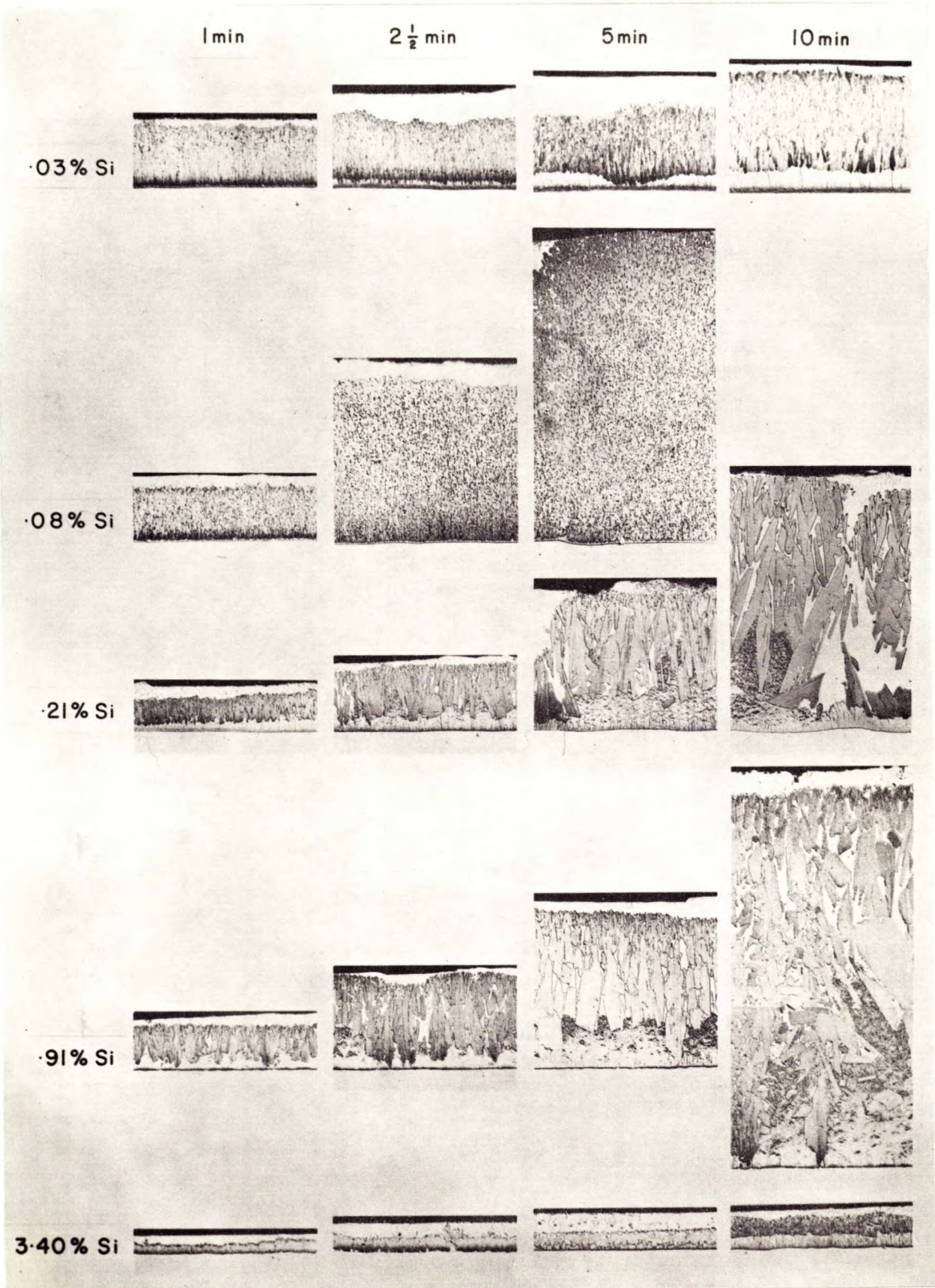


Figure 9. Microstructures of coatings on phosphorus-containing alloys at 450°C (840°F). Magnification reduced to 185X in reproduction.





1 unit = 5.4 μ

Figure 10. Microstructures of coatings on silicon-containing alloys at 450°C (840°F). Magnification reduced to 185X in reproduction.



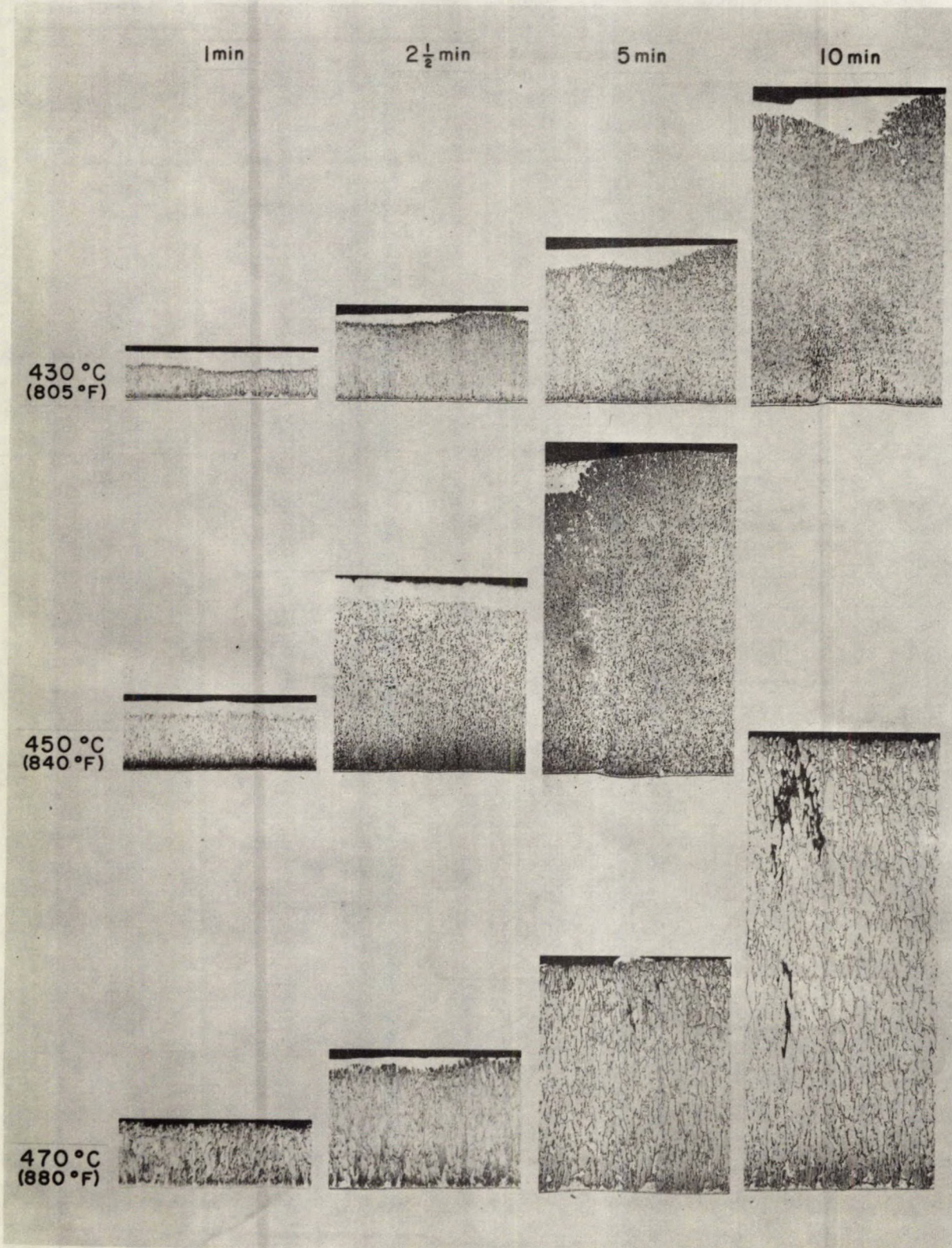


Figure 11. Microstructures of coatings on 0.08% Si alloy at different temperatures. Magnification reduced to 185X in reproduction.



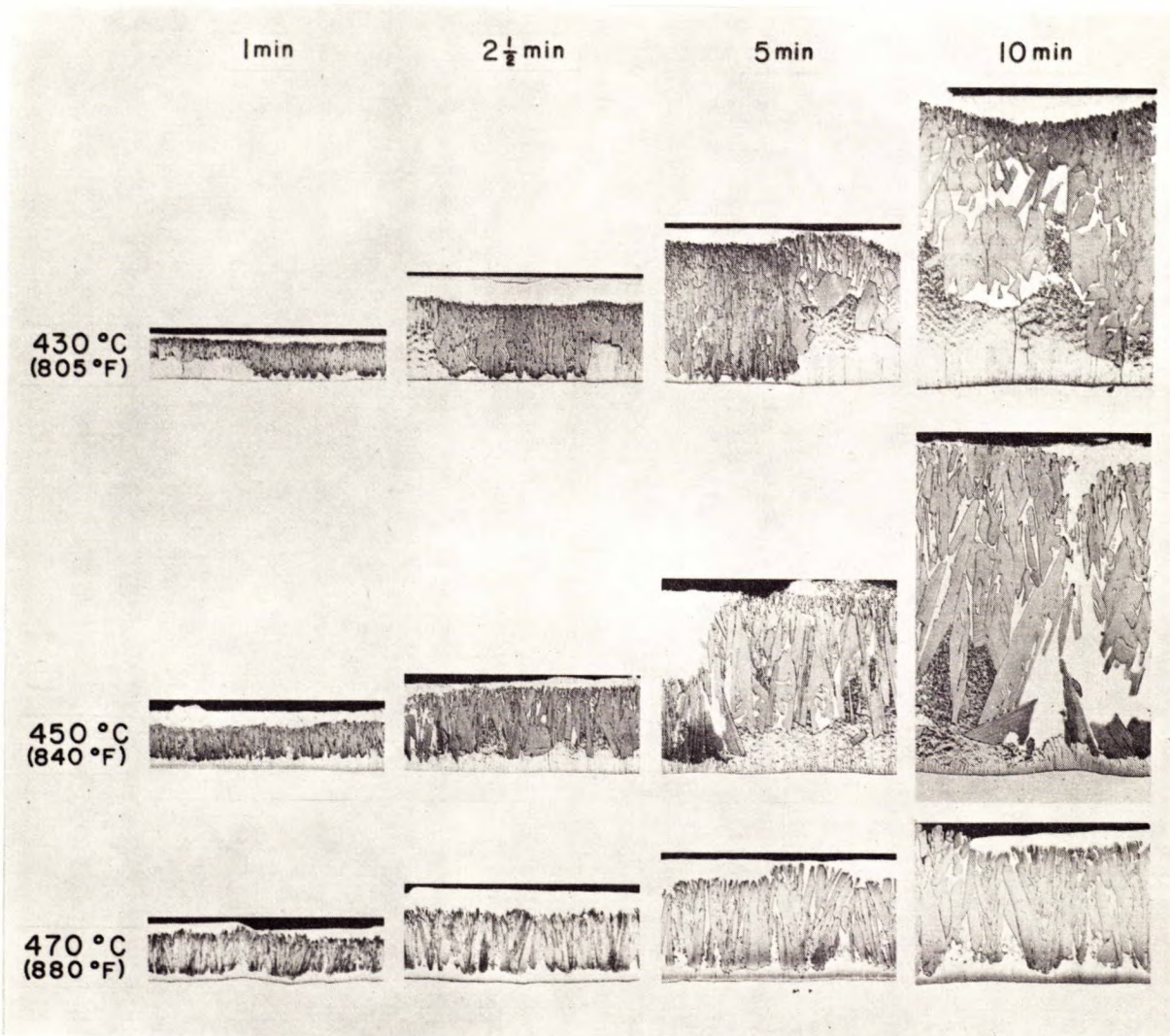


Figure 12. Microstructures of coatings on 0.21% Si alloy at different temperatures. Magnification reduced to 190X in reproduction.

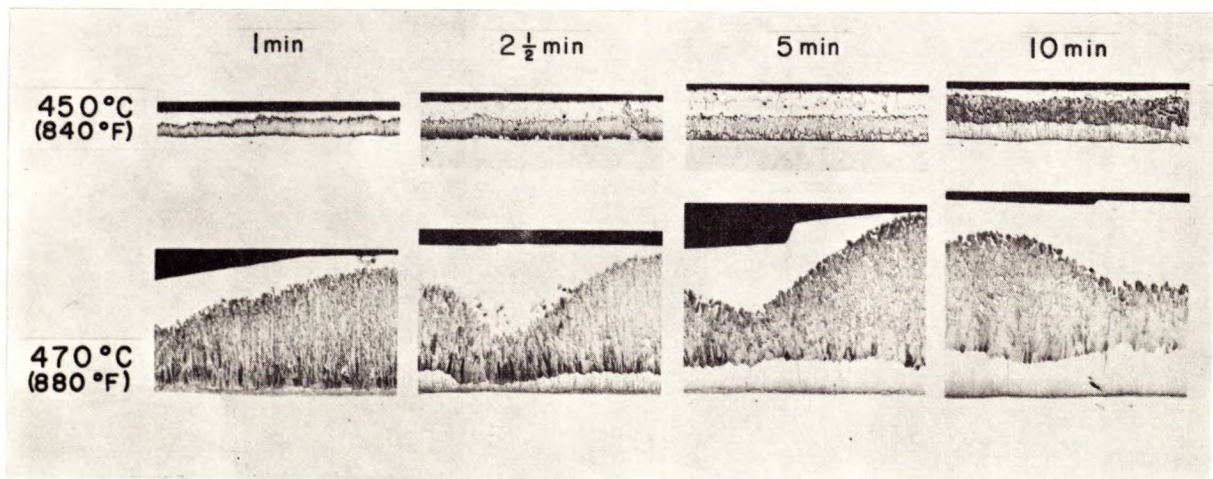


Figure 13. Microstructures of coatings on 3.4% Si alloy at different temperatures. Magnification reduced to 185X in reproduction.



